

## Highlights

### **Note on Using Singular Value Decomposition to Solve Diluted Pore Networks**

Ilan Ben-Noah, Juan J. Hidalgo, Marco Dentz

- Singular value decomposition is a highly efficient method to solve the flow equation in diluted pore network models
- Singular value decomposition can be used to locate singular points and clusters
- Singular value decomposition is extremely robust, allowing near-percolation threshold estimation

# Note on Using Singular Value Decomposition to Solve Diluted Pore Networks

Ilan Ben-Noah<sup>a,b</sup>, Juan J. Hidalgo<sup>a</sup>, Marco Dentz<sup>a</sup>

<sup>a</sup>*Institute of Environmental Assessment and Water Research (IDAEA) Spanish National Research Council (CSIC) Barcelona Spain.*

<sup>b</sup>*Department of Environmental Physics and Irrigation Institute of Soil Water and Environmental Sciences The Volcani Institute Agricultural Research Organization Rishon LeZion Israel*

---

## Abstract

Diluted pore networks or networks that are obtained directly from image analysis (e.g., CT scans of rock samples) are commonly used to evaluate flow through multiphase and complex porous media. These networks are often subjected to singular points and regions, that is, isolated sub-networks that are not connecting the inlet and outlet. These regions impair the invertibility of the Laplacian matrix and affect the accuracy and robustness of the pore network models. Searching and eliminating these singularities is commonly done by preconditioning or searching algorithms like breadth-first search (BFS) or depth-first search (DFS) that are time-consuming and computationally expensive. Here, we suggest using the Singular Value Decomposition (SVD) to simultaneously locate and eliminate isolated regions, and solve the flow equation. In this technical note, we briefly describe the SVD method and demonstrate its utility in solving the flow equation of different networks and dilution degrees. We show that the SVD is extremely robust, allowing exact solutions up to the percolation threshold. Moreover, we compare pore network solutions of images with and without singular regions to demonstrate how effective SVD is in locating and eliminating the singular regions while keeping the same solution in the relevant domain.

---

## 1. Introduction

Conceptualization of the media as a pore network (rather than a bundle of capillaries) goes back to the work of Fatt [1], where at its simplest form, it conceptualizes the

media as a lattice of conductors ( $g$ ), disregarding the pore shape. More complex (and realistic) pore network models relate the bonds' geometry to their conductance [2]. Regardless of the conductance values and connectivity, pore network models (PNM) commonly use a set of linear equations that can be represented by the Laplacian (or Kirchhoff matrix, which is a matrix representation of a graph).

$$\mathbf{L} \cdot \mathbf{P} = \mathbf{0}, \quad (1)$$

where  $\mathbf{P}$  is the vector of pressures at all sites of the network,  $\mathbf{L} = \mathbf{D} - \mathbf{G}$  is the weighted Laplacian matrix. It is given by the difference of the degree matrix  $\mathbf{D}$  and the conductance matrix  $\mathbf{G}$ . The degree matrix is a diagonal matrix that contains the degrees of each node, that is  $D_{ik} = \delta_{ik} \sum_{[ji]} g_{ij}$ . The weight matrix contains the conductances between connected sites  $G_{ij} = g_{ij}$  and 0 else. The pressure boundary conditions used here are implemented by defining  $\mathbf{L}'$  such that  $L'_{ij} = L_{ij}$  for all sites  $i$  that are not, and  $L'_{ij} = \delta_{ij}$  for all sites  $i$  that are in the inlet or outlet boundaries such that

$$\mathbf{L}' \cdot \mathbf{P} = \mathbf{b}, \quad (2)$$

where the vector  $\mathbf{b}$  on the right side of Eq. (2) contains the boundary conditions. We assign the pressure  $b_j = p_0$  at the sites  $j$  at the inlet boundary and  $b_j = 0$  else.

For regular networks,  $\mathbf{L}$  is a diagonal matrix of a  $Z + 1$  band, where  $Z$  is the coordination number, i.e., the number of interconnected junctions. For this case,  $\mathbf{L}$  is an invertible (non-singular) matrix, and (1) can be solved directly to obtain  $\mathbf{P}$ . However, in many types of media and flow problems, the media cannot be conceptualized by a set of regular media. For example, it is useful to conceive a porous media's imbibition (or drainage) process as the activation (deactivation) of conductors on a grid [3]. In this context, percolation theory deals with the effects of the occupation probability ( $p$ ) of either lattice bonds or lattice sites on the formation of a lattice-spanning, connected cluster, on the probability of the bonds (or sites) to belong to the conducting backbone of this cluster, and on its conductance [4, 5, 3, 6].

After randomly eliminating bonds (assigning zero values to pore conductances,  $g$ ),  $\mathbf{G}$  may now contain isolated sites and clusters that may cause numerical problems since they lead to a singular or ill-conditioned matrix. It should be mentioned that

this issue is not restricted to diluted regular networks but rather a general issue in any system of linear equations with singular values, such as models derived directly from image analysis of porous and fractured media. The challenge of addressing this singularity issue was raised in many PNM. For example, Raouf and Hassanizadeh [7] used a searching algorithm to find and remove all ill-connected sites and clusters. More recently, Guo et al. [8] used a "seed filling method" that iteratively goes over all pixels at the pores peripheral (and increases it) to evaluate its connectivity. These algorithms are time-consuming and computationally expensive. In this contribution, we suggest using the Singular Value Decomposition (SVD) method as a superior way to eliminate the singular points of the matrix. The method is shortly explained in section 2.1.

## 2. Methods

### 2.1. Singular Value Decomposition

The Singular Value Decomposition (SVD) is a well-known method for solving homogenous linear equations and low-rank matrix approximations. Its utility spans many fields, such as signal processing, image analysis, and astrodynamics, to name a few. SVD is the factorization of the matrix  $\mathbf{L}$  into the product of three matrices of the form

$$\mathbf{L} = \mathbf{U}\mathbf{\Sigma}\mathbf{V}^T \quad (3)$$

where the columns of  $\mathbf{U}$  and  $\mathbf{V}$  are orthonormal and the matrix  $\mathbf{\Sigma}$  is diagonal with positive real entries ( $\sigma$ ), called the singular values of  $\mathbf{L}$ . The singular values, and more specifically the number of non-zero  $\sigma_i$ , is the rank of the matrix  $\mathbf{L}$ , i.e., the number of linearly independent columns of  $\mathbf{L}$ . The columns of  $\mathbf{V}$  (termed the right singular vectors of  $\mathbf{L}$ ), and also the columns of  $\mathbf{U}$  (the left singular vectors), always form an orthogonal set with no assumptions on  $\mathbf{L}$ . This means that the inverse of the invertible matrix  $\mathbf{L}$  follows

$$\mathbf{L}^{-1} = \mathbf{V}\mathbf{\Sigma}^{-1}\mathbf{U}^T \quad (4)$$

For the case where  $L$  is a singular matrix (i.e., at least one  $\sigma_i = 0$ ), we follow the low-rank matrix approximation [9], in which the pseudoinverse of the diagonal matrix is determined by setting  $\Sigma_{i,i}^{-1} \approx \widetilde{\Sigma}_{i,i}^{-1} = \frac{1}{\sigma_i}$ . Then, the infinite (and extremely large)

values of  $\tilde{\Sigma}^{-1}$ , corresponding to zero (or very small, practically zero up to some numerical accuracy)  $\sigma_i$ , are eliminated (replaced by zeros). This somewhat counter-intuitive process is known as the Eckart-Young theorem [9]. Thus, the pressure distribution is

$$\mathbf{P} \approx \mathbf{V}\tilde{\Sigma}^{-1}\mathbf{U}^T\mathbf{b} \quad (5)$$

The permeability  $k$  of a medium is defined as the flux of a viscosity unit that a unit pressure gradient ( $\nabla P$ ) will invoke [10]

$$k = \frac{q_m\mu}{|\nabla P|} = \frac{q_m\mu}{\rho g_c}. \quad (6)$$

The flux  $q_m$  is given in terms of the volumetric flow rate, or discharge rate  $Q$  as  $q_m = \frac{Q}{A}$ , which can be measured at any medium cross-section ( $A$ ). The relative permeability ( $k_r$ ) is defined as the fraction of the actual permeability from the saturated intrinsic permeability of the media ( $k_s$ ).

The main advantage of the SVD is that it does not require any matrix preconditioning and can be used for singular or invertible matrices. At the same time, this method is robust and accurate, as demonstrated in this note.

## 2.2. Image analysis

The accuracy of the SVD solution approximation by comparing the results of a random network constructed from an image of a manufactured 2D milifluidic device during multiphase flow before (Figure 1a) and after (Fig. 1b) processing the image to exclude the non-percolated disconnected phase. The non-processed image (Fig. 1a) contains many disconnected regions of different sizes. The small regions are formed by the wetting liquid phase films surrounding the grains (pillars), while the larger clusters are formed by the entrapment of the liquid phase by the non-wetting gas phase. Conversely, the processed image (Fig. 1b) does not include singular regions. The image processing was conducted using the MATLAB image analysis toolbox [11]. The image analysis for pore partitioning follows the methodology presented in [12]. The construction of the detailed network follows the methodology presented in [13].

For the network constructed from the non-processed image, the flow equation is then solved using SVD (Eq. 4), and the pressure at the sites ( $P$ ) is evaluated (5). For

the network of the processed image, the flow equation was solved using SVD (Eq. 4) and again by directly reversing the Laplacian matrix (Eq. 2) for comparison.

### 2.3. Diluted network

The SVD's robustness, that is, its ability to solve the flow equation at bond occupation probabilities close to the percolation threshold, is evaluated. To this end, we use SVD to solve the steady flow equation on two types of diluted lattices: i) Hexagonal 2D lattice ( $Z_s = 3$ ), and ii) Square 2D lattice ( $Z_s = 4$ ) at different occupation probabilities. For simplicity, in this stage, we use a dimensionless analysis with a uniform conductance field (with  $g = 1$ ), a unit voxel size ( $\Delta x = 1$ ), and a hundred bonds in each side of the lattice  $N_{sq} = N_{hex} = 100$ , and a unit pressure gradient ( $P(0) = L, P(L) = 0$ ), where  $L$  is the length of the domain in the main flow direction ( $L_{sq} = \Delta x N_{sq}, L_{hex} = \frac{3\Delta x N_{hex}}{4}$ , when the hexagonal lattice is oriented with the long diagonal in the main flow direction).

In each realization, we start with a fully saturated grid ( $Z = Z_s$ ). Then, the grid is diluted to obtain the occupation probability ( $p_b$ ). The  $p_b$  is related to the mean coordination number  $\langle Z \rangle$  through  $p_b = \frac{\langle Z \rangle}{Z_s}$ . The dilution method applied here follows a simplification to the protocol described by [7]. Each bond is randomly assigned with a dilution (or elimination) number (between 0 and 1). Then, all bonds with an elimination number larger than  $p_b$  are assigned zero conductivity.

Then, for each realization, the flow equation (Eq. 5) is solved using SVD (Eq. 4). Here, we keep a record of the number of singular points and define the singularity frequency ( $p_\sigma$ ) as the number of singular points normalized by the number of bonds (lattice junctions).

## 3. Validation and Demonstration

In this section, we validate and demonstrate SVD capabilities in two relevant aspects: accuracy and robustness. The flow rate distribution (Figure SF1 in the supplementary material) and pressure distribution of the pore network obtained from the non-processed image (Fig. 1c) at the relevant percolated pore space are similar to the

ones obtained at the processed image (Fig. 1d). The singular disconnected regions attain a zero pressure value. Moreover, the entire lattice relative permeability ( $k_r$ ) is very similar for the processed and non-processed image (about 0.2% difference), the  $k_r$  of the processed image using SVD (Eq. 4) and direct inverse (Eq. 2) is the same (difference  $\frac{k^{SVD}-k^{inv}}{k^{SVD}} < 10^{-11}$ ). These minor differences demonstrate the accuracy of SVD, and validity of the low rank matrix approximation.

The robustness of the SVD, i.e., its ability to solve the flow equation described by a low-rank matrix, is tested using diluted hexagonal and square lattices. The percolation probability ( $p_p$ ) is the media's probability of obtaining a sample spanning percolation. Here, we evaluate  $p_p$  as the relative number of realizations with a relative conductivity ( $k_r$ ) value larger than an extremely small value ( $10^{-10}$ ) that accounts for numerical accuracy. The physical minimal value of  $k$  can be evaluated by the extreme case of a tortuosity equals the number of sites, that is  $min(k) = \frac{1}{N_s}$ , which for our case obtains a minimum of  $5 \cdot 10^{-5}$  for the square lattice. This means that any smaller value is the result of a numerical truncation error. The theoretical bond percolation thresholds of the Hexagonal ("honeycomb") and square grids are respectively  $1 - 2\sin(\frac{\pi}{18}) \approx 0.6527$ , and  $\frac{1}{2}$  [3]. As expected, these values are in very good agreement with the occupation ( $p_b$ ) values in which the  $p_p$  equals 0.5 (Figure 2a). The slight variation in the observed values from the theoretical ones is due to the finite lattices ( $N = 100$ ) and the finite number of realizations ( $R = 50$ ). The SVD is extremely robust, obtaining physically reasonable values as long as the lattice is percolated. The effect of the occupation probability ( $p_b$ ) on the relative conductivity (Figure 2b) presents a linear relation far from the percolation threshold and some non-linear relation near the threshold until it reduces to zero below the percolation threshold. This is in accordance with the literature [14, 15]. The variance of the  $k_r$  values between realizations, visible by the width of the box plot and bars, is not linear, with a zero (trivial) variance at saturation and below the percolation threshold and a large variance in the intermediate values. The singularity frequency (Figure 2c) decreases with the increase in the  $p_b$ . Interestingly, at bond percolation threshold values ( $p_b = 0.5$  and  $\approx 0.65$  for square and hexagonal), the  $p_\sigma$  is about 0.05, which is well below the site percolation threshold of  $\approx 0.59$  and  $\approx 0.70$  for square and hexagonal grids [3]. This illustrates the significant differences

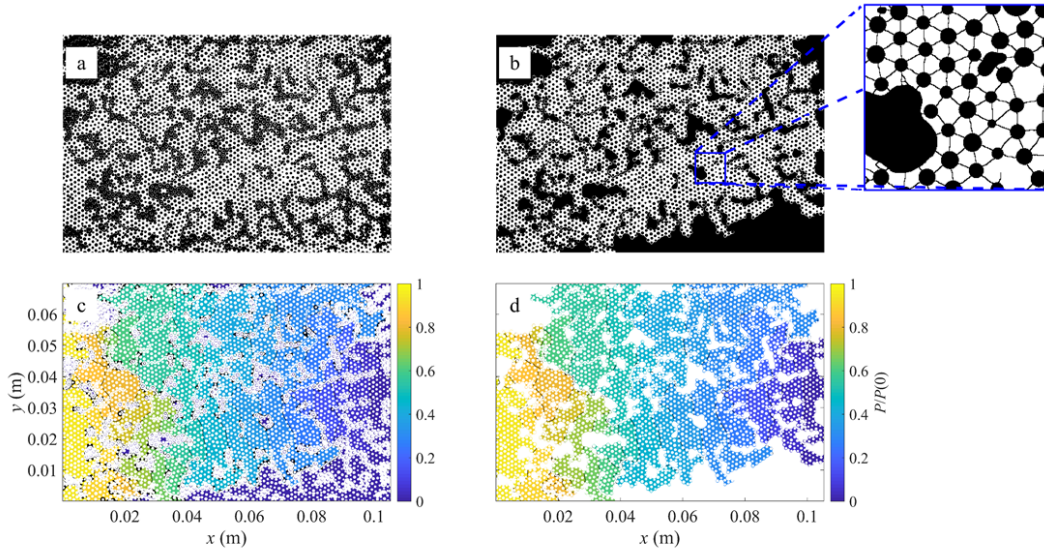


Figure 1: a) Binary image of the liquid phase (white) configuration during multi-phase flow through a microfluidic device (image provided by Yves Méheust). b) Binary image of the percolated and continuous liquid phase (white) in the small plot, the partitioned liquid-filled pore space in a zoom-in section (blue square). c) Pressure distribution in the pores using SVD to solve the non-processed image (a), singular regions are assigned with a value of 0. d) Pressure distribution (not using SVD) in the pores of the processed image (b).

between bond and site percolation processes, which are relevant to multiphase flow models but will not be discussed further in this study's scope.

#### 4. Conclusion

Singular value decomposition (SVD) is a robust, fast, simple, and accurate method to solve low-rank matrices. These traits are vital for solving diluted grids or image-derived pore-network models. Moreover, efficient codes for SVD are embedded in popular platforms such as MATLAB and Python. Despite that, SVD is under-used for solving pore-network models.



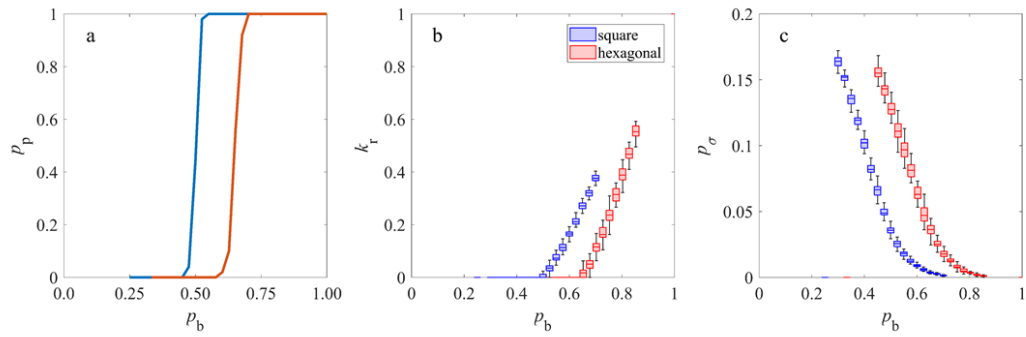


Figure 2: The effect of the occupation probability ( $p_b$ ) on: a) The percolation probability ( $p_p$ ); b) The relative lattice permeability ( $k_r$ ); and c) the singularity frequency ( $p_\sigma$ ), for square (blue) and hexagonal (red) lattices. Lattices with one hundred (100) bonds in each main direction and fifty (50) realizations at each  $p_b$  value are used for this analysis.

## **acknowledgments**

The authors thank Yves Méheust for the image of the milifluidic device. I.B.N, M.D. acknowledge funding from the European Union’s Horizon 2020 research and innovation programme under the Marie Skłodowska-Curie grant agreement No. HORIZON-MSCA-2021-PF-01 (USFT). I.B.N. , J.J.H. and M.D. acknowledge the support of the Spanish Research Agency (10.13039/501100011033), Spanish Ministry of Science and Innovation through grants CEX2018-000794-S and HydroPore PID2019-106887GB-C31. J.J.H. acknowledges the support of the Spanish Research Agency (10.13039/501100011033), the Spanish Ministry of Science and Innovation and the European Social Fund “Investing in your future” through the “Ramón y Cajal” fellowship (RYC-2017-22300).

## **5. Open Research**

No data was used in this research.

## **References**

- [1] I. Fatt, The network model of porous media, *Transactions of the AIME* 207 (1956) 144–177.
- [2] M. Sahimi, *Flow and transport in porous media and fractured rock: from classical methods to modern approaches*, John Wiley & Sons, 2011.
- [3] A. G. Hunt, M. Sahimi, Flow, transport, and reaction in porous media: Percolation scaling, critical-path analysis, and effective medium approximation, *Reviews of Geophysics* 55 (2017) 993–1078.
- [4] B. Berkowitz, R. P. Ewing, Percolation theory and network modeling applications in soil physics, *Surveys in Geophysics* 19 (1998) 23–72.
- [5] S. R. Broadbent, J. M. Hammersley, Percolation processes: I. crystals and mazes, in: *Mathematical proceedings of the Cambridge philosophical society*, volume 53, Cambridge University Press, 1957, pp. 629–641.

- [6] D. Stauffer, A. Aharony, Introduction to percolation theory, CRC press, 2018.
- [7] A. Raoof, S. M. Hassanizadeh, A new method for generating pore-network models of porous media, *Transport in porous media* 81 (2010) 391–407.
- [8] X. Guo, K. Yang, H. Jia, Z. Tao, M. Xu, B. Dong, L. Liu, A new method of central axis extracting for pore network modeling in rock engineering, *Geofluids* 2021 (2021) 1–20.
- [9] G. W. Stewart, On the early history of the singular value decomposition, *SIAM review* 35 (1993) 551–566.
- [10] M. Muskat, H. Botset, Flow of gas through porous materials, *Physics* 1 (1931) 27–47.
- [11] The MathWorks Inc., Matlab version: 9.13.0 (r2022b), 2022. URL: <https://www.mathworks.com>.
- [12] I. Ben-Noah, J. J. Hidalgo, M. Dentz, Efficient pore space characterization based on the curvature of the distance map, 2024. [arXiv:2403.12591](https://arxiv.org/abs/2403.12591).
- [13] I. Ben-Noah, J. J. Hidalgo, M. Dentz, Evaluation of different network models in variably saturated media, 2024. [arXiv:?????.?????](https://arxiv.org/abs/?????.?????)
- [14] S. Kirkpatrick, Percolation and conduction, *Reviews of modern physics* 45 (1973) 574.
- [15] S. P. Friedman, L. Zhang, N. A. Seaton, Gas and solute diffusion coefficients in pore networks and its description by a simple capillary model, *Transport in porous media* 19 (1995) 281–301.